



## Research Article

Yhors Ciro\*, John Rojas, Cristian J. Yarce, and Constain H. Salamanca\*

# Preparation, Characterization and Rheological Behavior of Glutathione-Chitosan Conjugates in Aqueous Media

<https://doi.org/10.1515/arh-2019-0010>

Received May 04, 2019; accepted Sep 05, 2019

**Abstract:** Glutathione-chitosan conjugates are adequate carriers for anticancer treatment due to their ability for inhibition of efflux pumps, improved mucoadhesivity and *in-situ* gelling. These conjugates were obtained via carbodiimide at different reaction times in order to get different thiolation degrees (*i.e.*, 4.4%, 5.1% and 7.0%) and their behavior in aqueous media at a pH of 4, 5 and 6 was assessed by measurements of hydrodynamic diameter, zeta potential and rheological analyses at a pH ranging from 4 to 6. Data examination was conducted by principal component analysis (PCA) which in turn explained 73.1% of data variability. All samples showed a Newtonian flow and thiolation rendered materials with a highly pronounced temperature-dependent behavior and a gel-like structure. In turn, the phase shift angle was the most prominent rheological change especially at a pH of 5.0 and 6.0 due to the formation of disulfide bonds. The thiolation degree was the most influential factor and it was inversely related to particle charge and consistency index.

**Keywords:** Aggregation-pH dependence, glutathione-chitosan conjugates, thiolation-rheology response

**PACS:** 87.14Df, 81.20Ka, 82.70Dd, 66.20.-d, 82.80 Yc

**\*Corresponding Author: Yhors Ciro:** University of Antioquia, School of Pharmaceutical and Food Sciences, Department of Pharmacy, 67 Street No. 53 - 108, Medellín, Colombia; Email: yhors.ciro@udea.edu.co

**\*Corresponding Author: Constain H. Salamanca:** Departamento de Ciencias Farmacéuticas, Facultad de Ciencias Naturales, Universidad Icesi, Calle 18 No. 122 -135, Cali 76003, Colombia; Email: chsalamanca@icesi.edu.co

**John Rojas:** University of Antioquia, School of Pharmaceutical and Food Sciences, Department of Pharmacy, 67 Street No. 53 - 108, Medellín, Colombia; Email: rojasca@gmail.com

**Cristian J. Yarce:** Departamento de Ciencias Farmacéuticas, Facultad de Ciencias Naturales, Universidad Icesi, Calle 18 No. 122 -135, Cali 76003, Colombia; Email: cjarce@icesi.edu.co

## 1 Introduction

Chitosan (CH) is a cationic polymer with biodegradable, biocompatible, and mucoadhesive properties, which have been the object of thousands of studies in diverse science fields. This material has been used to create composites, microcapsules, nanoparticles, and cross-linked materials. For instance, thiolation of the CH structure confers particular properties such as *in-situ* gelling, mucoadhesivity, cell permeation and inhibition of efflux pumps [1]. This ultimate parameter is relevant for the treatment of cancer, especially where resistant lines are involved. Moreover, these polymers also known as thiomers are formed by the covalent attachment of ligands such as 6-mercaptopenicilaminic acid, cysteine 2-imiothiolane, N-acetyl-penicilamine, 4-mercaptobenzoic acid, N-acetyl-cysteine, glutathione, and thioglycolic acid [2], and their *in-situ* gelling properties differ on the magnitude of the gel-sol transition time. The latter property is crucial on formulations intended for mucoadhesive drug delivery generating a stable rapid and gel-like structure avoiding the removal mechanisms on mucosa, and hence extending the residence time of the loaded drug [3]. Currently, only the study of Sakloetsakun and collaborators has explored the rheological behavior of just one type of thiolated chitosan. In this case, they synthesized thioglycolic acid-CH conjugates followed by oxidation and assessed the frequency sweep response. As a result, oxidation promoted the generation of disulfide bonds, reduced the amount of free thiol moieties, decreased the sol-gel transition time and loss tangent. Conversely, oxidation enhanced the values of dynamic viscosity of these conjugates [4].

Since the anion form of the thiol moiety is very stable the thiolation reaction must be carried out at acidic pH (*i.e.*, <5) in order to avoid the oxidation of thiol groups [5]. Conversely, the use of catalysts such as N-hydroxysuccinimide allows for a reaction to take place at a pH range from 5.0 to 6.5 and extended times up to 24 h [6]. Up-to-date, there are no studies about the effect of larger reaction times and thiolation degree on the aqueous characterization of thio-



lated chitosan. Therefore, the goal of this study is to characterize and evaluate the rheological behavior in solution of three glutathione-CH conjugates obtained at reaction times ranging from 24h, 72h and 120h corresponding to thiolation degrees of 4.4%, 5.1% and 7.0%, respectively. Therefore, it is worthwhile to explore and evaluate the performance of these highly thiolated materials at a pH range (4-6) and temperature (37°C) similar to those of the human body and infer their aqueous behavior for the delivery of bioactive agents. In turn, the release rate of these agents will be affected by the thiolation degree of the glutathione-chitosan conjugates.

## 2 Experimental

### 2.1 Materials

CH with a degree of acetylation of 25% (lot STBF8219V), *N*-(3-Dimethylaminopropyl)-*N'*-ethylcarbodiimide hydrochloride (carbodiimide) (lot, BCBR6841V, purity >97%), glutathione (lot SLBQ4892V, purity >98%) and *N*-hydroxysuccinimide (lot MKBX1364V, purity 98%) were purchased from Sigma Aldrich Co (St. Louis, Missouri, USA). Sodium hydroxide (lot B1315798639), HCl (lot K45147217 349), deuterium oxide (D<sub>2</sub>O, lot S5725666, purity ≥ 99.9%) and acetic acid (lot K41575763) were obtained from Merck (Darmstadt, Germany). Sodium chloride (lot 13843802) was purchased from Scharlau (Barcelona, Spain).

### 2.2 Synthesis of thiolated chitosan

Approximately, 100 mL of 1% (w/v) solution of deacetylated CH (DCH with a deacetylation degree of 85% and 477 kDa MW, obtained by microwave-assisted alkaline hydrolysis for 2h, using additive cycles of 5 min) was prepared in 1% (v/v) acetic acid at a pH of 6.0 (adjusted with a 5N NaOH solution). Subsequently, the solution was mixed with 5g of glutathione, carbodiimide and *N*-hydroxysuccinimide to get a final concentration and pH of 200 mM and 6.0, respectively. This mixture was kept under constant stirring for 24, 72 and 120h at 25°C. Thereafter, the mixture was dialyzed in 5 mM HCl solution using membranes having a cut-off MW of 12 kDa. The dialysis process was then repeated with 5 mM HCl/1% (w/v) NaCl, followed by treatment with 1 mM HCl in 24h cycles. Thiolated materials were then lyophilized at -45°C and 0.04 bar (Model, EYELA

FDU-1100, Rikakikai Co., Tokio, Japan) and stored in a desiccator under silica gel at 25°C until further testing.

#### 2.2.1 <sup>1</sup>H-NMR Characterization and quantification of the thiolation degree

The <sup>1</sup>H-NMR spectra of polymers dissolved in D<sub>2</sub>O acidified with acetic acid were recorded on a Bruker Ascend III HD spectrometer using a 5 mm TXI probe and operated at 600 MHz. The MestRenova<sup>®</sup> software (Mestrelab Research S.L., v.12) was used for collecting the spectra, whereas the Peakfit<sup>®</sup> software (Seasolve, Inc, v.4.12) was used to calculate the area under the curve. The thiolation degree (TD) was determined as follows:

$$TD = \frac{A_{SH}}{A_{total}} * 100\% \quad (1)$$

Where,  $A_{SH}$  corresponds to the integral of SH signal at ~1 ppm and  $A_{total}$  is the complete area under the curve in the <sup>1</sup>H-NMR spectrum.

### 2.3 Particle size and zeta potential analyses

The effect of media pH on particle size and zeta potential of thiolated materials was assessed on a Zetasizer (Nano ZSP, Malvern Instrument-UK) coupled with an auto-titrator. A 1M NaOH solution was used as a titration agent. Polymer solutions of 2 mg/mL were tested at a pH ranging from 4 to 6. Measurements were performed in triplicate at 25°C.

### 2.4 Rheological analysis

The rheological tests were performed on a Rheometer (MCR 92, Anton Paar, Graz, Austria) coupled with either a cone-plate or concentric cylinder, accordingly. Approximately, 500 mg of each material was dissolved in 50 mL of 1% (v/v) acetic acid solution. The initial pH of all solutions was 4.0 and subsequently 10.0 mL aliquots were taken followed by pH adjustment at 5.0 and 6.0 with a 3M NaOH solution. All measurements were performed at a temperature of 37.0 ± 0.3°C once reached this condition.

#### 2.4.1 Flow behavior

Samples were analyzed using a concentric cylinder geometry (26.66 mm, diameter) coupled with the Rheocompass<sup>®</sup> (v.1.20, Anton Paar) software. Three frequencies intervals

were employed: (i) an ascending phase of 0.01-100 Hz, followed by 100 Hz for 1 min and (iii) a deceleration phase of 100-0.01 Hz. The dwell time at each phase was 1 min and 10 measurements were recorded for interval. Approximately, 15 mL of each sample was poured in the measuring cup (C-CC27/T200/XL and 28.934 mm diameter) and data were fitted to the Herschel-Bulkley, Oswald and Bingham models as follows:

$$\tau = t_0 + K * (\dot{\gamma})^n \quad (2)$$

$$\tau = K * (\dot{\gamma})^n \quad (3)$$

$$\tau = t_0 + \eta_b * (\dot{\gamma}) \quad (4)$$

Where,  $\tau$ ,  $t_0$ ,  $K$ ,  $\dot{\gamma}$ ,  $\eta_b$  and  $n$  correspond to the shear stress, yield stress, the consistency index, shear rate and flow behavior index, and Bingham viscosity, respectively.

#### 2.4.2 Viscoelastic properties

The linear-viscoelastic region was determined from 0.01 to 100% of strain employing a cone-plate geometry ( $1^\circ$  angle and 50 mm diameter, gap 0.150 mm) and 2 mL of sample. The frequency sweep was executed from 0.1 to 628 Hz at a 1% strain using a cone-plate system and 21 points of storage ( $G'$ ), loss moduli ( $G''$ ) were recorded, along with their crossover points (PC).

#### 2.4.3 Temperature sweep

The temperature sweep was evaluated using 15 mL of sample and a concentric cylinder geometry at a strain and frequency of 0.1% and 1 Hz, respectively. A heating phase was conducted from 25 to 80°C at a rate of 2.9°C/min followed by a cooling phase from 80 to 25°C at a rate of 1.6°C/min.

### 2.5 Statistical analysis

The statistical analysis was performed using the Minitab<sup>®</sup> software (v. 17, Minitab<sup>®</sup> Inc., State College, PA, USA). Further, a one-way ANOVA test was used for data analysis and  $p$ -values <0.05 were considered as significant. Moreover, a multivariate analysis known as PCA was used to determine the relationship of the variables studied.

## 3 Results and discussion

### 3.1 Synthesis of thiolated chitosan

Thiolated DCH was generated by the inclusion of glutathione to the DCH backbone forming an amide linkage between the carboxylic acid moiety on the glycine residue of glutathione and amine moiety of the C-2 of DCH. Carbodiimide was used to activate the carboxylic moieties forming an O-urea derivative, which reacted with the amine moieties of DCH. However, these CH conjugates are easily hydrolyzed and thus, *N*-hydroxysuccinimide allowed for the formation of a more stable ester derivative increasing the thiolation degree of DCH. Therefore, the O-acylisourea derivatives are transformed into a *N*-hydroxysuccinimide-activated carboxylic acid, forming a zero-length branching with the amine groups of DCH [7] (Figure 1).

#### 3.1.1 <sup>1</sup>H-NMR characterization and quantification of the thiolation degree

The <sup>1</sup>H-NMR spectra of DCH and thiolated derivatives are shown in Figure 2. The DCH spectrum shows signals at 2.9-3.1 ppm attributed to the hydrogen proton of the glucosamine subunit. The peaks at 3.4-4.0 ppm represent the H<sub>3-6</sub> anomeric protons of the carbohydrate ring [8]. Moreover, the glutathione spectrum reveals signals at 1.3-1.4 ppm ascribed to the SH proton, and the signals at 1.8-1.9 ppm are shown as a shoulder of the main of acetic acid peak, attributed to the H<sub>12-13</sub> protons. Further, the signals at 2.3-2.5, 3.7-3.8, 3.9-4.0 and 4.4-4.5 are due to the H<sub>10-11</sub>, H<sub>14</sub>, H<sub>2-3</sub> and H<sub>8</sub> protons, respectively [9]. Conversely, the spectra of thiolated materials showed a peak at 1.0-1.2 ppm due to the SH proton of glutathione [10] and other typical signals of glutathione as mentioned previously. Further, the resulting thiolation degree of these materials was 4.4%, 5.1% and 7.0% and these samples were labeled as CH-SH-24h, CH-SH-72h and CH-SH-120h indicating that the reaction time had a significant effect on the incorporation of glutathione onto the DCH backbone.

### 3.2 Determination of particle size and zeta potential

The zeta potential and hydrodynamic diameter vs pH profile of thiolated materials is depicted in Figure 3.

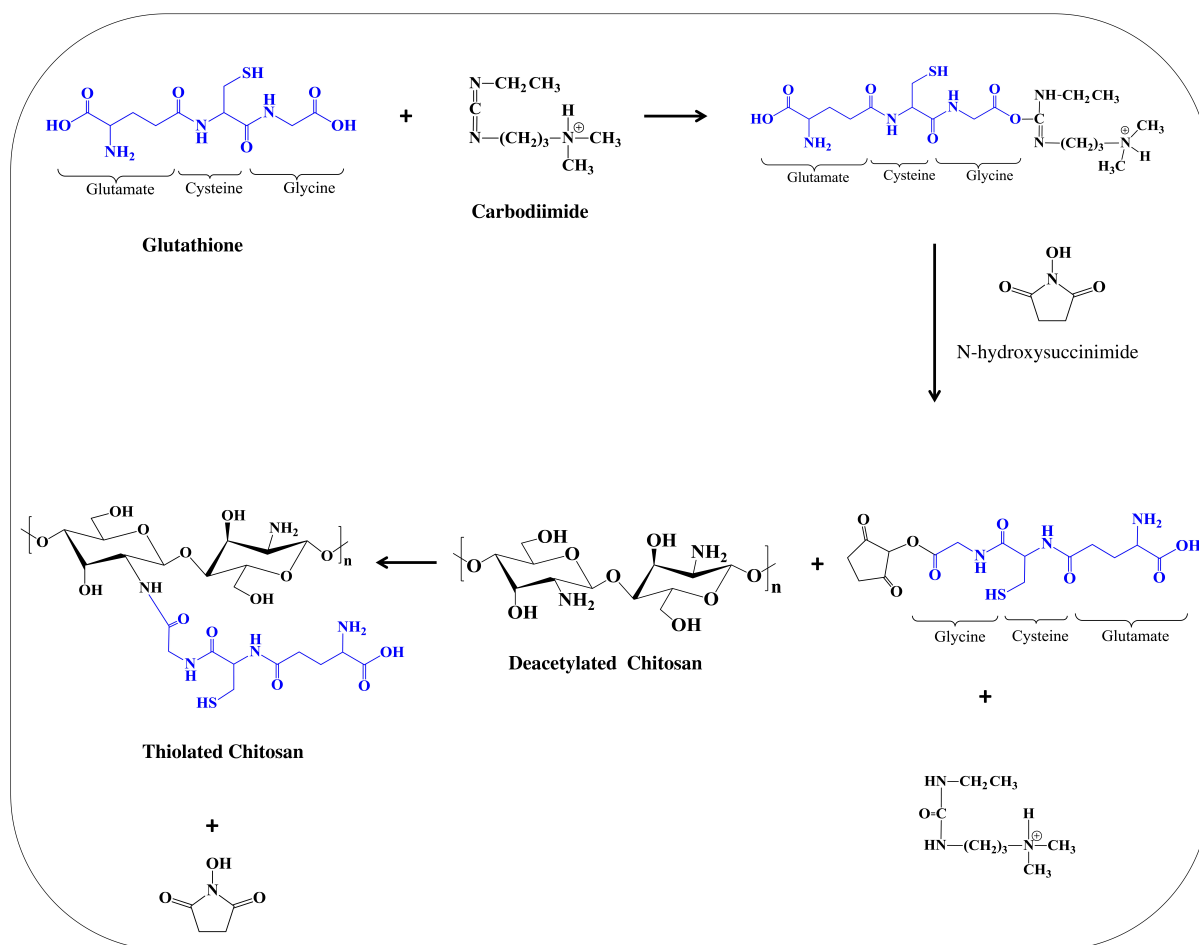


**Figure 1:** Presumptive reaction scheme for the formation of thiolated chitosan.

In all the cases, the zeta potential (PZ) decreased with the increasing pH. This phenomenon is explained by the loss of positive density charge of amine moieties (changing from  $NH_3^+$  to  $NH_2$ ) in DCH [11]. On the other hand, the magnitude of PZ of thiolated derivatives was insignificant as compared to that of DCH due to the ionization of the carboxylic acid moiety of the glutathione, which conferred a negative charge within the polymer neutralizing the amine moieties. For this reason, as the thiolation degree increased, the magnitude of PZ decreased due to a greater presence of carboxylic groups coming from glutathione. Likewise, as the pH increased the hydrodynamic diameter ( $D_H$ ) of DCH increased. This is explained by the synergistic effect due to (i) the inter-chain attractive interactions such as hydrogen bonds and (ii) hydrophobic interactions due to the decrease of electrostatic repulsion allowing for interchain interactions forming larger agglomerates. Furthermore, with the decrease of protonation DCH became insoluble resulting in a  $D_H$  increase [12]. Nevertheless, the  $D_H$  of thiolated materials showed an opposite behavior at

pH of 5.0 and 6.0 resulting in lower values due to the oxidation of free thiol groups to disulfide bonds decreasing the volume occupied by the polymer chains. Moreover, DCH was obtained by microwave-assisted alkaline hydrolysis rendering a product with chains having different lengths due to the random breakdown of glycosidic bonds in the CH structure, resulting in a non-homogeneous  $D_H$ . This fact was corroborated by the high values (>0.5) of polydispersity index (PDI) listed in Table 1.

### 3.3 Rheological analysis

#### 3.3.1 Flow behavior

The flow curves of the samples are presented in the Figure 4. These profiles show a lineal increment of shear stress as the shear rate increases. Conventionally, the testing mode for assessing the hysteresis behavior of a material implies conducting at least one ascending and de-

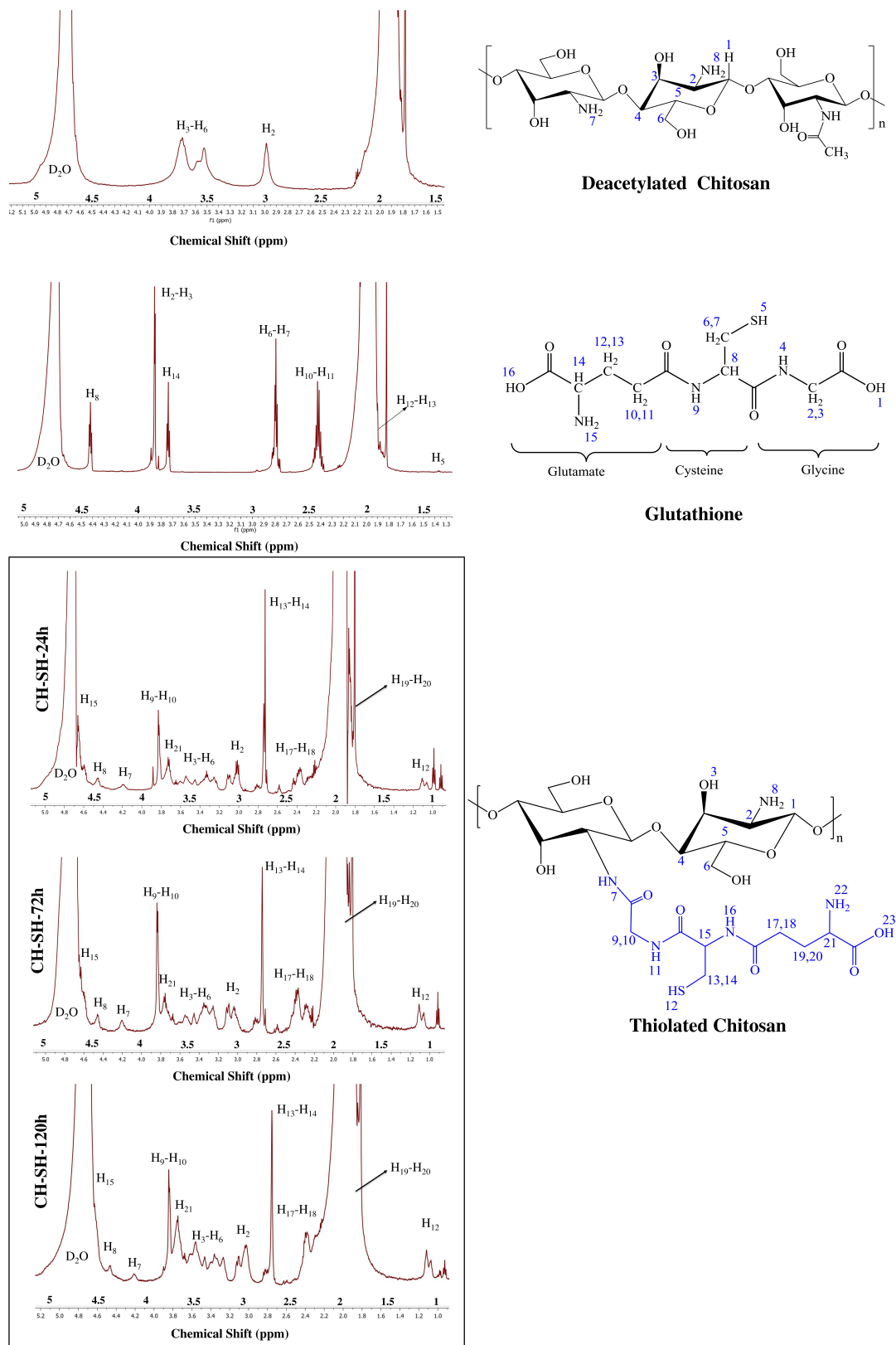
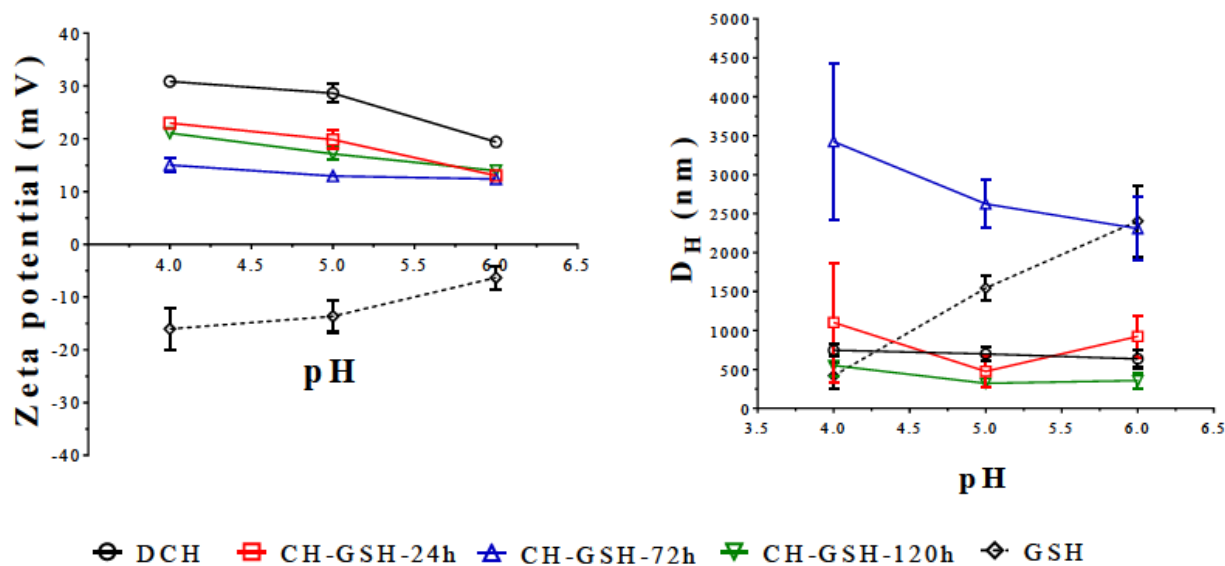


Figure 2: <sup>1</sup>H-NMR spectra of deacetylated chitosan, glutathione and thiolated derivatives.



**Figure 3:** Zeta potential (left) and hydrodynamic diameter (right) of deacetylated chitosan, glutathione and thiolated derivatives in solutions having different pH.

**Table 1:** Physical characterization of aqueous thiolated chitosan dispersions included in the PCA analysis.

| DT (%) | pH | PZ (mV) | $D_H$ (nm) | PDI   | PSA ( $^\circ$ ) | $G'$ (Pa) | $G''$ (Pa) | PC (Hz) | AH (%) | n    | K (Pa*s) | to (Pa)  |
|--------|----|---------|------------|-------|------------------|-----------|------------|---------|--------|------|----------|----------|
| 0      | 4  | 30.9    | 745.6      | 0.783 | 0.61             | 0.082     | 0.066      | 158     | 0.62   | 1    | 0.026    | 0.002    |
| 4.4    | 4  | 23      | 1102.5     | 0.698 | 0.38             | 0.125     | 0.037      | 15.8    | 1.49   | 1.07 | 0.001    | 0        |
| 5.7    | 4  | 15      | 3424.7     | 0.906 | 0.84             | 0.068     | 0.044      | 251     | 0.23   | 1.06 | 0.002    | 0        |
| 7      | 4  | 21.1    | 551.2      | 0.759 | 0.97             | 0.031     | 0.025      | 251     | 0.02   | 0.94 | 0.004    | 0.000024 |
| 0      | 5  | 28.6    | 697.9      | 0.876 | 0.95             | 0.02      | 0.031      | 0.441   | 2.06   | 0.99 | 0.011    | 0.001    |
| 4.4    | 5  | 19.8    | 475.4      | 0.805 | 0.31             | 0.115     | 0.038      | 39.8    | 1.04   | 0.95 | 0.001    | 0        |
| 5.7    | 5  | 12.9    | 2624       | 0.917 | 0.89             | 44.119    | 33.88      | 39.8    | 0.25   | 1.41 | 0.002    | 0.006    |
| 7      | 5  | 17.1    | 321.2      | 0.55  | 0.94             | 0.057     | 0.028      | 398     | 0.27   | 0.97 | 0.001    | 0        |
| 0      | 6  | 19.4    | 634.3      | 0.779 | 0.59             | 0.064     | 0.055      | 1.58    | 0.84   | 0.98 | 0.02     | 0        |
| 4.4    | 6  | 13      | 923.3      | 0.7   | 0.43             | 0.101     | 0.05       | 100     | 0      | 1.25 | 0.0004   | 0.004    |
| 5.7    | 6  | 12.4    | 2309.7     | 0.987 | 0.37             | 0.101     | 0.051      | 0       | 1.45   | 1.09 | 0.001    | 0.001    |
| 7      | 6  | 13.9    | 356.8      | 0.558 | 0.2              | 0.056     | 0.029      | 513     | 0.12   | 1.12 | 0.001    | 0.002    |

PZ: Zeta potential,  $D_H$ : Hydrodynamic volume, PDI: polydispersity index, PSA: Phase shift angle,  $G'$ : Storage modulus,  $G''$ : Loss modulus, PC: Crossover points, AH: Hysteresis area, n: Flow behavior index, K: Consistency index, to: Yield stress.

scending cycle. We employed an intermediate and sustained step of 100 Hz to disrupt the alignment of the polymer structure and assess its ability to recover the original structure once the shear rate is ceased. Moreover, the table 1 lists the parameters obtained from the Herschel-Bulkley model. This model showed a better fitting to the experimental data ( $r^2 > 0.97$ ) than the Oswald model due to the presence of an extra term (the yield stress factor) which accounts for the high viscosity value once a shear force is applied. On the other hand, the Bingham model did not show a good curve fitting since this model showed impre-

cise stress values at low shear rates. The “n” factor indicates the flow type behavior, when it takes the value of 1 the material behaves as a Newtonian fluid. On the contrary, if n is lower or larger than 1 indicates a shear thinning and shear thickening behavior, respectively [13]. Therefore, in most samples is expected a Newtonian behavior since they exhibited n values ranging from 0.94 to 1.12. Thus, the shear rate favored the disruption of entangled polymer coils, but re-entanglement occurred simultaneously mitigating the effect of shear rate [14]. Moreover, at a pH of 5.0 and 6.0 this index moved to values larger than 1.0 for

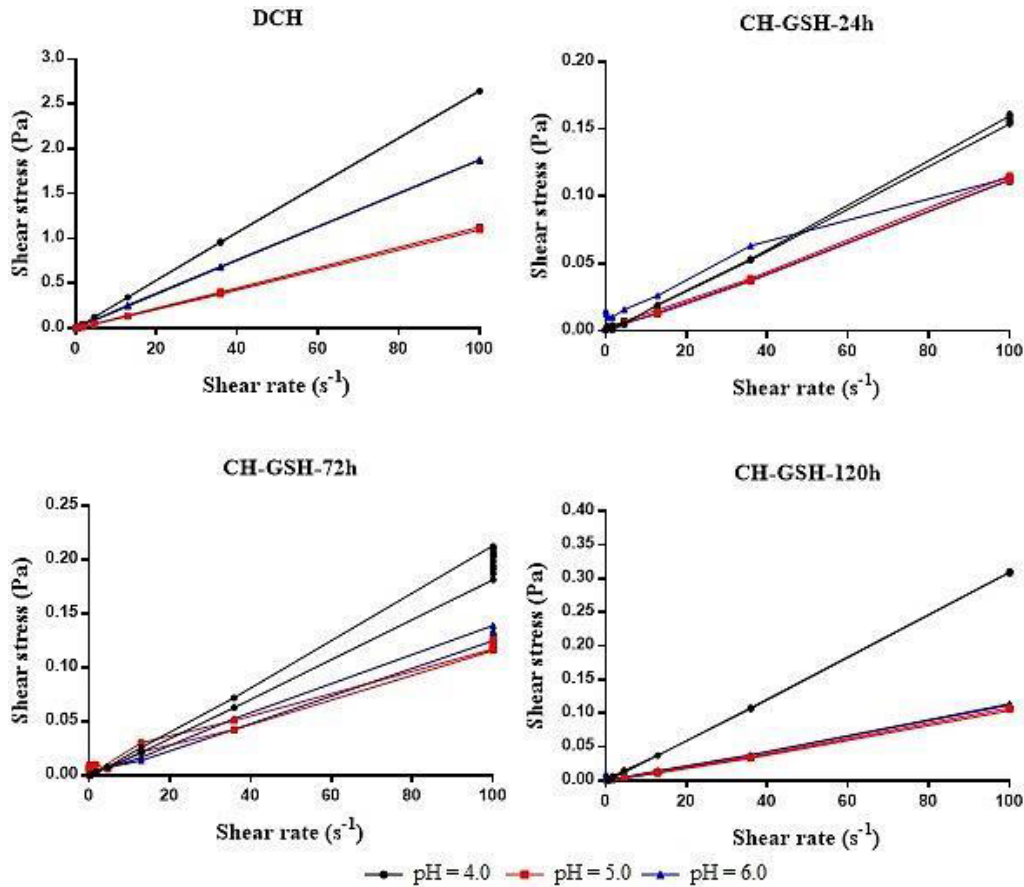


Figure 4: Flow curves in terms of shear stress for polymeric solutions.

CH-SH-24h and CH-SH-72h due to the formation of disulfide bonds. However, the flow behavior of DCH showed a concentration-dependent character as proved by Hwang and Shin. Thus, at concentrations larger than 1% (%w/v) it showed a pseudoplastic flow due to a restriction on the movement of individual chains as a consequence of the high molecular density, and thus, the lag time for new entanglement formation increased [15]. Solutions of chitosan composites have shown a similar behavior. For instance, Singh and Kumari developed CH/starch composites and found that as the CH level increased, the aqueous behavior deviated from Newtonian to a pseudoplastic flow [16]. On the other hand, the consistency index ( $K$ ) of thiolated conjugates was lower than those of DCH independent of pH. This effect can be attributed to the amorphization increment upon thiolation (the crystallinity degree for DCH was ~45%, whereas those found for thiolated derivatives was <15%). This phenomenon in turn, limits entanglement driving movement in the chains upon shear rate initiation. Likewise, as the thiolation degree increased, the “ $K$ ” factor increased. Conversely, the values of yield stress as expected remained low due to the prevalent Newtonian flow

exhibited for most samples. This fact was corroborated by the hysteresis areas (AH), as calculated from the ratio of the increasing and decreasing segments of the flow curve, which were lower than 5% (Table 1) indicating a predominant Newtonian flow. The coefficients of determination ( $r^2$ ) ranged from 0.9711 to 0.9998, indicating that the Herschel-Bulkley model described the experimental data satisfactorily.

### 3.3.2 Viscoelastic properties

In general, the viscoelastic region of samples ranged from 0.1 to 10% of strain independent of the medium pH. Figure 5 depicts the effect of frequency on the  $G'$  and  $G''$  modules at each pH value. In the case of DCH at pH of 4.0  $G''$  was larger than  $G'$  indicating the prevalence of the viscous component, whereas at higher frequencies  $G'$  was larger than  $G''$  indicating a breakdown of the arrangement of the polymer chains in solution. Moreover, as pH increased  $G'$  was larger than  $G''$  at low frequencies mainly due to interactions such as hydrogen bonds, London and

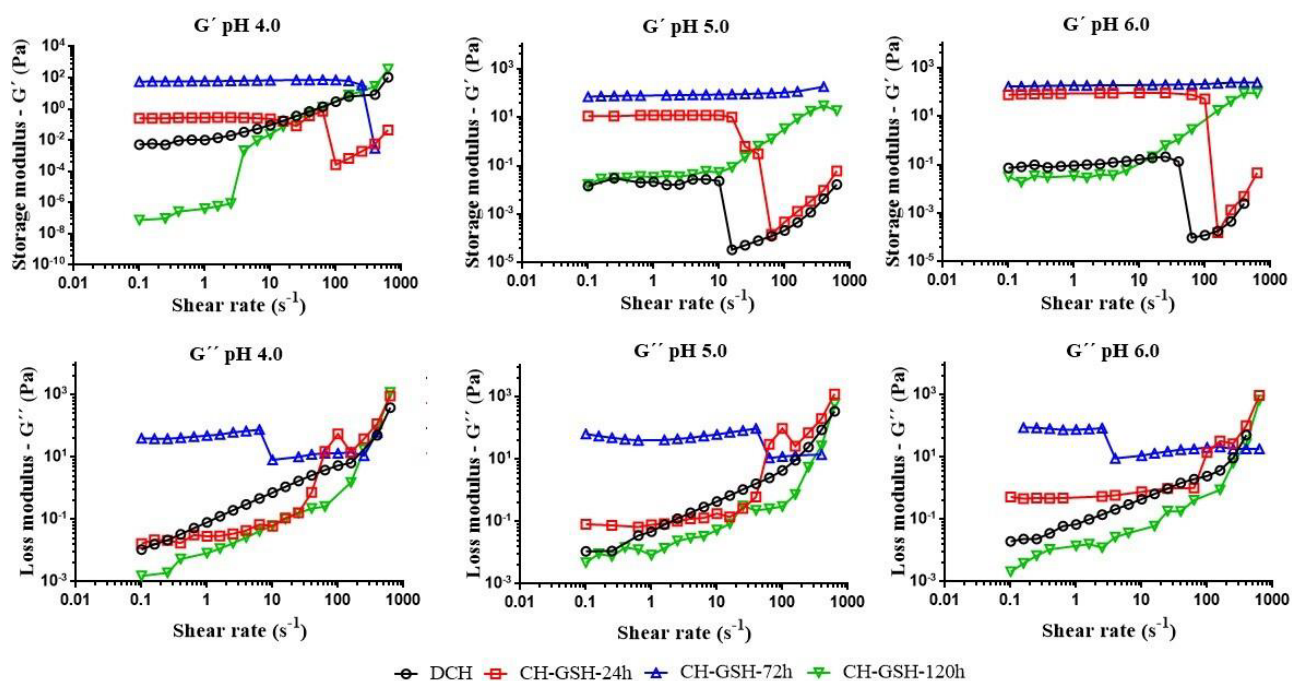


Figure 5: Rheological behavior in terms of storage ( $G'$ ) and loss moduli ( $G''$ ) for polymeric solutions.

Van der Waals forces as explained above, causing a major tension in the chain segments and the formation of multiple entanglements rendering a predominant elastic behavior [14]. Further,  $G'$  surpassed  $G''$  in thiolated CHs independent of pH and frequency indicating a solid-like behavior, attributed to higher polymer chain entanglements due to their lower zeta potential as compared to DCH indicating minor electrostatic repulsions and major interactions such as hydrogen bonds and hydrophobic attractions upon inclusion of GSH. Likewise, as the pH increased, the difference in magnitude between  $G'$  and  $G''$  increased in thiolated derivatives indicating a more pronounced elastic component presumably due to the formation of new disulfide bonds between chains. Thus, as the thiolation degree increased the frequency at which the intersection points in the modules also augmented along with  $G'$ . Interestingly,  $G'$  of CH-SH-72 at a pH of 6.0 was not influenced by the frequency sweep. The formation of disulfide bonds as reflected by the  $G'$  increment has been verified in studies where thiolated derivatives of CH (2-iminothiolane and thioglycolic acid conjugates) were incubated at 37°C for 6 h and periodically tested by a frequency sweep. Therefore, the different incubation periods promoted the formation of disulfide bonds due to the oxidation of free thiol groups. As a result, the  $G'$  increased as the incubation time proceeded and concomitantly the content of free thiol groups decreased [17, 18].

### 3.3.3 Temperature sweep

Table 2 lists the  $G'$ ,  $G''$  and phase shift angle (PSA) as resulted from the heating and cooling cycles for all samples at different pH. There were statistically significant differences ( $p < 0.05$ ) for  $G'$  at a pH of 6.0, particularly for thiolated derivatives. Therefore, the values of  $G'$  during the cooling phase were higher than those obtained at the heating phase since thermal treatment favored the oxidation of free thiol groups into disulfide bonds creating a more condensed structure in the polymer. As a result, PSA decreased during the cooling phase indicating a gel-like behavior due to crosslinking of chains by disulfide bonds conferring an ordered three-dimensional arrangement [19]. On the other hand, when the temperature increased the flexibility of DCH chains increased in response to the increment in the kinetic energy upon heating resulting in torsion of glycosidic linkages [20]. Moreover, DCH only showed a gel-like behavior at a pH of 6.0 as it is evidenced in the Figure 6.

### 3.4 Multivariate analysis

The PCA correlation analysis (PC1, PC2 and PC3) indicates that 73.1% of variability in the data set is explained by the first three components. The raw data used for this analysis are presented in the Table 1. The variance for PC1, PC2 and





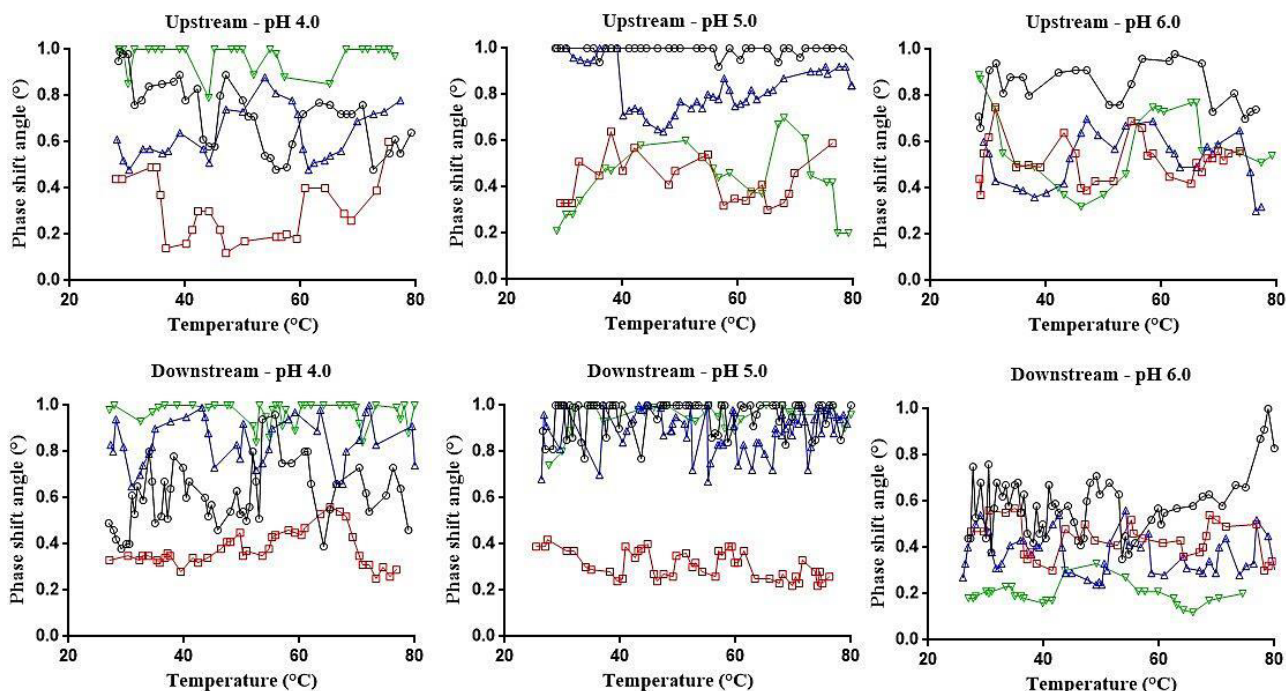


Figure 6: Phase shift angle as a function of temperature for polymeric solutions.

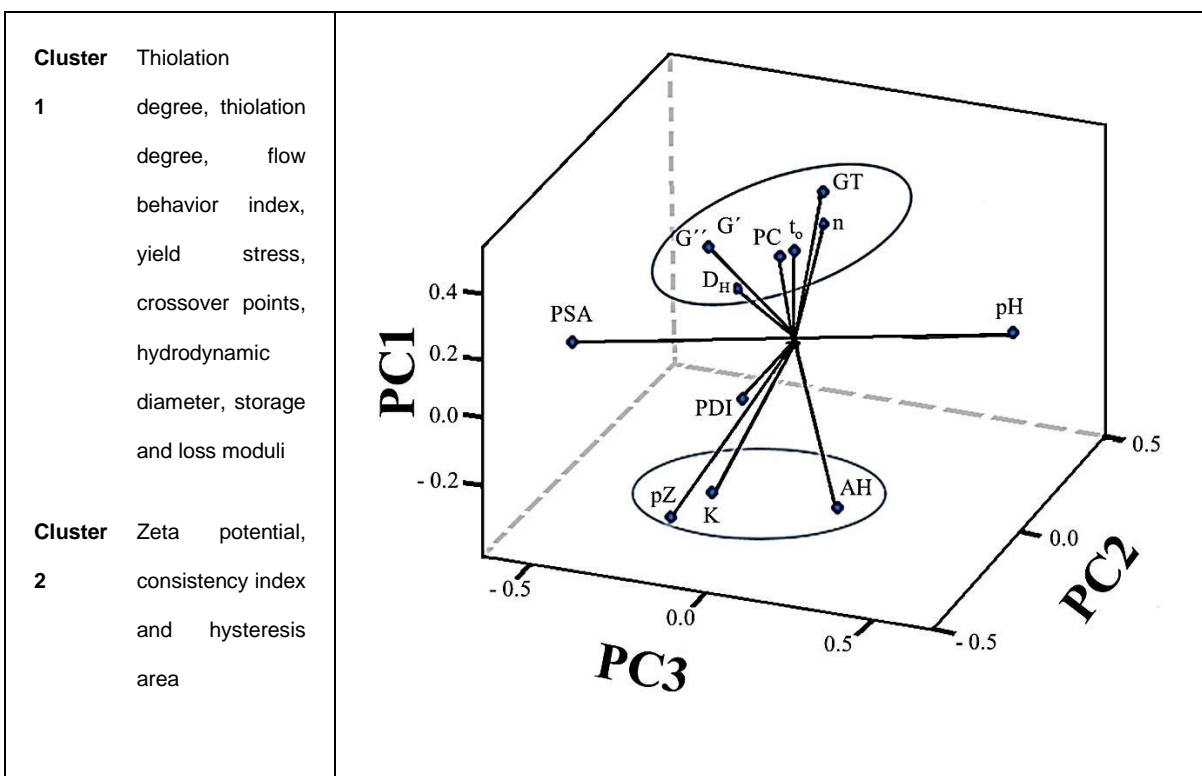


Figure 7: Loading plot for representative properties of thiolated materials. PC1: 35.0%, PC2: 24.2% and PC3: 13.9%. AH: hysteresis area,  $D_H$ : hydrodynamic diameter, GT: thiolation degree,  $G'$ : storage modulus,  $G''$ : loss modulus, K: consistency index, n: flow behavior index PC: crossover point, PDI: polydispersity index, pH: medium pH, PSA: phase shift angle, PZ: zeta potential,  $t_0$ : yield stress.

PC3 was about 4.6, 3.1 and 1.8, respectively. Figure 7 depicts the loading plot of the PCA exhibiting two clusters for data variability.

The PC1 vector relates  $G'$  and  $G''$  moduli with flow behavior index, yield stress and  $D_H$ . The PC2 vector relates the thiolation degree with crossover points, but where inversely related with the consistency index, hysteresis area, zeta potential and PDI index. The PC3 shows an inverse relationship of the pH and hysteresis area pair with phase shift angle and crossover points. The scores for PC1, PC2 y PC3 can be briefly expressed as:

$$\text{PC1} : 0.396G' + 0.395G'' + 0.429n + 0.373t_0 \\ - 0.336PZ + 0.282D_H$$

$$\text{PC2} : 0.407GT + 0.459PC - 0.327AH - 0.306k \\ - 0.274PZ - 0.424pdi$$

$$\text{PC3} : 0.584pH - 0.579PSA - 0.292PC + 0.295AH$$

Moreover, from the correlation analysis is deduced that thiolation degree was inversely correlated with the consistency index ( $r = -0.845$ ) and zeta potential ( $r = -0.702$ ). In turn, the zeta potential was correlated with the consistency index ( $r = 0.700$ ). Likewise,  $G'$  and  $G''$  were highly correlated ( $r = 1.000$ ) and, at the same time they were correlated with the flow behavior index ( $r = 0.774$ ) and yield stress ( $r = 0.765$ ).

It is worthwhile mentioning that a moderate thiolation degree (5.1%) provides a solid-like behavior independent of the shear rate at the pH range between 4 and 6. This interesting result is the key for the controlled release of bioactive ingredients upon oral administration since these molecules should withstand the pH and peristaltic movement of the GI tract. Likewise, thiolated derivatives showed a major gel-like behavior implying a better modulation of the release rate of these compounds. Moreover, if needed the synthesis method could be modified by adding heating and thawing processes in order to target specific sites in the GI tract.

## 4 Conclusion

Thiolation of DCH rendered products that presented a major elastic component. These derivatives were susceptible to the increment of temperature and pH, which in turn favored the rise of the storage modulus and the formation of a gel-like structure due to the oxidation of thiol groups to disulfide bonds. The thiolation degree was the most influential parameter on the physical behavior of this material in solution. Furthermore, the Newtonian flow of DCH was

not affected by thiolation, but thiolated products lost the innate thermoreversibility of DCH. Future studies, should deal with the effect of temperature on gelling time and assess the effect of thiolation degree on the controlled release of key bioactive compounds.

**Acknowledgement:** This study was funded by the Colombian Institute of Science (Colciencias) through the grant No. 727-2015. CHS and CJY grateful to Icesi University for the internal research grant No. 041380. The authors would like to especially thank the committee for the development of research (CODI) of University of Antioquia and its Sustainability Strategy Program (2018-2019) for their financial support.

## References

- [1] Laffleur F., Berknop-Schnuřch A., Thiomers: promising platform for macromolecular drug delivery, *Futur. Med. Chem.* 4, 2012, 2205–2216.
- [2] Bonegel S., Berknop-Schnuřch A., Thiomers – From bench to market, *J. Control. Rel.* 195, 2014, 120–129.
- [3] Cho I.S., Cho M.O., Jang B.S., Cho J.K., Park K.H., Kang S.W., Huh K.M., Synthesis and characterization of thiolated hexanoyl glycol chitosan as a mucoadhesive thermogelling polymer, *Biomater. Res.* 22, 2018, 1–10.
- [4] Sakloetsakun D., Hombach J.M., Bernkop-Schnuřch A., In situ gelling properties of chitosan–thioglycolic acid conjugate in the presence of oxidizing agents, *Biomaterials.* 30, 2009, 6151–6157.
- [5] Ciro Y., Rojas J., Salamanca C., Thiolated chitosan: A promising strategy for improving the effectiveness of anticancer drugs, In *Analytical and Pharmaceutical Chemistry*, SMGroup, 2017.
- [6] Mojarradi H., Coupling of substances containing a primary amine to hyaluronan via carbodiimide-mediated amidation, 2010.
- [7] Kafedjiiski K., Foęer F., Werle M., Berknop-Schnuřch A., Synthesis and in vitro evaluation of a novel chitosan-glutathione conjugate, *Pharm. Res.* 22, 2005, 1480–1488.
- [8] Pereria A.G.B., Muniz E.C., Hsieh Y.L., <sup>1</sup>H NMR and <sup>1</sup>H-13C HSQC Surface Characterization of Chitosan-Chitin Sheath-Core Nanowhiskers, *Carbohydr. Polym.* 123, 2015, 46–52.
- [9] Kaiser L.G., Marjańska M., Matson G.B., Iltis I., Bush S.D., Soher B.J., Mueller S., Young K., <sup>1</sup>H MRS detection of glycine residue of reduced glutathione in vivo, *J. Magn. Reson.* 202, 2010, 259–266.
- [10] Li J., Shu Y., Hao T., Wang Y., Quian Y., Duan C., Sun H., Lin Q., Wang C., A chitosan-gluthathione based injectable hydrogel for suppression of oxidative stress damage in cardiomyocytes, *Biomaterials.* 34, 2013, 9071–9081.
- [11] Hussain Z., Katas H., Mohd Amin M.C., Kumolosasi E., Buang F., Sahudin S., Self-assembled polymeric nanoparticles for percutaneous co-delivery of hydrocortisone/hydroxytyrosol: An ex vivo and in vivo study using an NC/Nga mouse model, *Int. J. Pharm.* 444, 2013, 109–119.
- [12] Saięd N., Aięder M., Zeta potential and turbidimetry analyzes for the evaluation of chitosan/phytic acid complex formation, *J. Food*

- Res. 3, 2014, 71–81.
- [13] Osswald T.A., Rudolph N., Generalized Newtonian Fluid (GNF) Models. In *Polymer Rheology: Fundamentals and Applications*, Hanser Publishers, Munich, 2014.
- [14] Duffy J., *Measuring the rheology of polymer solutions*, 2015.
- [15] Hwang J.K., Shin H.H., Rheological properties of chitosan solutions, Korea-Australia. *Rheol. J.* 12, 2000, 75–179.
- [16] Singh V., Kumari K., Rheological behaviour of chitosan-starch solution, *Asian. J. Chem.* 25, 2013, 9817–9821.
- [17] Bernkop-Schnürch A., Hornof M., Zoidl, Thiolated polymer-sthiomers: Synthesis and in vitro evaluation of chitosan-2-iminothiolane conjugates, *Int. J. Pharm.* 260, 2003, 229–237.
- [18] Hornof M.D., Kast C.E., Bernkop-Schnürch A., In vitro evaluation of the viscoelastic properties of chitosan-thioglycolic acid conjugates, *Eur. J. Pharm. Biopharm.* 55, 2003, 185–190.
- [19] Krauland A.H., Hoffer M.H., Bernkop-Schnürch A., Viscoelastic properties of a new in situ gelling thiolated chitosan conjugate, *Drug. Dev. Ind. Pharm.* 31, 2005, 885–893.
- [20] Torres M.A., Beppu M.M., Arruda E.J., Viscous and viscoelastic properties of chitosan solutions and gels, *Brazilian. J. Food. Technol.* 9, 2006, 101–108.